行政院國家科學委員會補助專題研究計畫成果報告

※※※※※※※※※※※※※※※※※※※※※※※※※※
※　　　　　　　　　　　　　　　　　　　　　　　　※
※　　　　種苗品質動態生長模式之研究　　　　　　　※
※　　　　　　　　　　　　　　　　　　　　　　　　※
※※※※※※※※※※※※※※※※※※※※※※※※※※

計畫類別：■個別型計畫　　□整合型計畫

計畫編號：NSC 89－2313－B－002－238

執行期間：89 年　08 月　01 日至　90 年　07 月　31 日

計畫主持人：陳 世 銘　台灣大學 生物產業機電工程學系

共同主持人：

計畫參與人員：謝 廣 文　中興大學 農業機械工程學系

陳 加 增　台灣大學 生物產業機電工程學系

李 明 達　台灣大學 生物產業機電工程學系

執行單位：台灣大學 生物產業機電工程學系

中　華　民　國　九十 年　十　月 三十一 日

行政院國家科學委員會專題研究計畫成果報告

種苗品質動態生長模式之研究

Development of Dynamic Growth Model toward Seedling Quality

計畫編號：NSC 89－2313－B－002－238
執行期間：89年 08月 01日至 90年 07月 31日

計畫主持人：陳世銘 台灣大學生物產業機電工程學系
計畫參與人員：謝廣文 中興大學農業機械工程學系
陳加增 台灣大學生物產業機電工程學系
李明達 台灣大學生物產業機電工程學系

中文摘要

本研究建立可以應用於種苗自動化栽培之動態生長模式。甘藍種苗於三個生長階段有關環境條件影響苗品質之生長實驗於台大人工氣候室進行。倒傳遞類神經網路用來分析實驗數據，並建立動態生長模式之策略，可以用來陳述生長環境因子（日溫、每日每穴盤之澆水量、每日累積日照量）與甘藍苗品質（累積乾物重）之關係。整合回饋機制與動態策略於類神經網路模式中，以彰顯種苗生長之歷史因子的重要性。本研究已成功建立了動態生長模式，其決定係數可達0.996，而誤差僅為 1.68%，模式並以育苗場之數據驗證過。動態生長模式之預測結果遠優於靜態生長模式，其預測誤差可減少 80% 之多（由 18.2% 降為 3.75%）。本研究建立之動態生長模式可應用於實際的種苗生產自動化栽培管理系統中，配合種苗生長環境之回饋控制，可有效的估測與控制種苗的品質。

關鍵詞：動態生長模式、類神經網路、種苗品質、環境條件

ABSTRACT

This study presents a dynamic growth model applicable to automated seedling cultivation. Experiments on the influence of environmental conditions on cabbage seedling quality during three growth stages were conducted in a phytotron, and a growth database was established. An error back propagation neural network was used to analyze experimental data and develop strategies for a dynamic growth model to simulate the relationship between environmental factors (temperature, water supply and daily radiation) and cabbage seedling

quality (cumulative dry matter of seedlings). A feedback algorithm and dynamic strategies were integrated into the neural network to reflect the strong importance of daily historical memory in seedling growth. The dynamic model was thus successfully developed with a coefficient of determination of 0.996 and error of 1.68%, and was verified using the data from nurseries. The dynamic model performed excellently in determining seedling growth, achieving superior results to static models. The error in predicting the cumulative dry matter resulting from seedling growth was reduced by about 80% (from 18.2% to 3.75% prediction error) when the dynamic growth model was used in place of the static model. This model not only gave a clear view of production management toward seedling growth, but also provided a basis for better environmental and quality control strategies.

Keywords: Dynamic Growth Model, Neural Network, Seedling Quality, Environmental Conditions.

INTRODUCTION

Many investigations have indicated that a growth model employing environmental controls can be applied to predict crop growth (Jones et al., 1989; Seginer et al., 1986). Several growth models have been developed for various crops, such as tomatoes (Jones et al., 1991), cucumbers (Nederhoff et al., 1989), lettuce (Marsh et al., 1987), and Bok-Choi (Shen and Chang, 1994). The growth model is a useful tool for investigating crop growth management and environmental control since it can predict the growing conditions according to environmental variable responses. However, the control settings of traditional crop growth models have certain limitations and constraints. Consequently, Jacobson et al. (1987) improved the growth model by introducing artificial intelligence.

A neural network is an artificial intelligence information management system that can simulate biological systems. Such a system can ascertain the training data inner rules that would be applied to new cases through the network calculations. The agricultural system is generally complicated, nonlinear, and difficult to control. A neural network can be used to establish a complicated predictive model for agricultural research. Several agricultural neural network applications have been attempted. Murase et al. (1992) developed a neural network model to estimate the maximum hoop stress produced in the skin of a tomato during cracking. Meanwhile, Seginer and McClendon (1992) employed a neural network to determine the optimum temperature for lettuce in a greenhouse. Furthermore, Elizondo et al. (1994) developed a neural network model to predict the flowering and physiological maturity of soybeans. Finally, Chen et al. (1999) evaluated sugar content in fruits by a near infrared method using a back propagation network, while Hsieh et al. (1999) adopted a neural network to investigate the relationship between environmental factors and cabbage seedling quality. All the above investigations demonstrate the feasibility of applying neural networks to agriculture. This study aims mainly to develop a dynamic growth model

applicable to automated seedling cultivation. This cabbage seedling growth model was used to simulate and analyze how environmental conditions influence seedling quality.

EXPERIMENTS AND ANALYSIS

The seedling cultivation period was divided into three growth stages, and the cumulative dry weight of the seedlings was measured on the last day of each stage. A growth curve was constructed using cubic spline functions based on experimental data and the average cumulative weight of dry matter without roots per plant (DW) was interpolated from the growth curve throughout the entire growth period.

1. Experimental Design

The seedling cultivation environmental variables included air temperature, water management, and daily radiation. Four controlled day temperatures (20°C, 25°C, 30°C, 35°C) were preset for the temperature control rooms in National Taiwan University's phytotron for seedling cultivation. The relative humidity in each control room was maintained at between 70% and 90%.

The temperature control rooms were divided into low temperature (20°C, 25°C) and high temperature (30°C, 35°C) sets. Four 128-cell plug trays were used to cultivate the cabbage seedlings in each growth room. Cabbage seedlings in the low temperature set were irrigated with 200, 400, 800, and 1200mL of water per plug tray daily, while 400, 800, 1200, and 1600mL of water was supplied to the high temperature set. The trays receiving 200 and 400mL of water were given the whole of their water allocation at 8 a.m., while those receiving 800, 1200, and 1600mL of water were given their water in two halves, at 8 a.m. and 4 p.m. The combination of temperature and water management resulted in sixteen treatments for each experiment.

The hourly PAR (Photosynthetically Active Radiation) was measured using an LI-110SA (LI-COR, Inc), and recorded by a Campbell Scientific 21X data logger. The summed total daily PAR represented the daily radiation.

In each experiment, the cultivation period lasted thirty days. Seedling cultivation is generally divided into three ten-day growth stages, the first ten days after sowing, then the eleventh to the twentieth day, and finally the twenty-first to the thirtieth days. The first growth stage includes germination, cotyledon and stalk growth, the second includes leaf growth, and the third was dominated by reinforcement (Huang, 1992).

The cumulative dry matter weight (DW) was served as the quality index for the growth model. Thirty seedlings from each treatment were randomly sampled and their cumulative dry matter weight without roots measured on the last day of each growth stage. The cumulative dry matter weight data from 30 seedlings per sampling was divided equally into two sets, one used for model training and the other for prediction. Six experiments were conducted in various seasons, and each experiment provided forty-eight combinations of growth environments (four temperature control conditions, four water management conditions, and three growth stages).

2. Seedling Growth Curves

Hsieh et al. (1999) showed that time was a major influence on seedling growth, and that seedling growth history was needed to explain the relationship between the growth environment and growth quality. Therefore, seedling growth curves were constructed to provide growth history information.

The DW was measured on the last day of each growth stage, with the DW on the first and second days after sowing being considered as zero (DW was zero for the part above the ground during germination) in each treatment. Each treatment had six data entries (including initial DW = 0) for each set of learning and testing samples. Meanwhile, the cubic spline function was employed to construct the growth curve, as presented in Fig. 1. The cubic spline equation is defined as follows (Gerald and Wheatley, 1999; MALAB, 1995):

$$y = a_i(x-x_i)^3 + b_i(x- x_i)^2 + c_i(x- x_i) + d_i$$

where y denotes the cumulative dry matter weight, x represents the days after sowing, and a_i, b_i, c_i, d_i are coefficients, i = the segment number, the segment 1 from x = 2 to x = 10, $x_1 = 2$, the segment 2 from x = 10 to x = 20, $x_2 = 10$, the segment 3 from x = 20 to x = 30, $x_3 = 20$.

The DW was interpolated for the other twenty-five days according to the growth curve. The data used to develop the growth model were from the fifth (the initial day of recording daily radiation) to the thirtieth day, including the experimental DW values on the tenth, twentieth and thirtieth days, and the interpolated values of DW for the other 23 days.

3. Model Establishment Procedure

The error back propagation neural network was adopted as the growth model herein (Fig. 2), and computer programs for neural network modeling were written using Turbo C++ 3.0. The models developed herein can make predictions within the ranges being investigated in the experiments, namely: 20–35°C for day air temperature, 200–1600mL for daily water supply per plug tray, 3.8–38.6 mole/m^2 for total daily radiation, and 0.38–225mg/seedling for DW on the preceding day (DW_{i-1}).

This work established static and dynamic growth models for cabbage seedlings. The neural network used was a dual-hidden layer structure with ten neurons per hidden layer. The key difference between the static and the dynamic models was the consideration of the time factor during the learning process. The static learning process was further divided into two types. Type I combined all the sample data from the six experiments and used just one neural network for learning. The input parameters of the neural network were day temperature (℃), daily water supply per plug tray (mL), total daily radiation (mole/m^2), growth stage and cumulative weight of dry matter per seedling on the preceding day (DW_{i-1}) (mg/seedling). Meanwhile, Type II combined only sample data from the same growth stage of six experiments. Three neural networks, one for each stage, were used for learning. The Type II neural network used four input parameters, day temperature, daily water supply per plug tray, total daily radiation and DW_{i-1}, because the three growth stages were clearly distinguished. Both neural networks used the measured DW as the

neural network target value (output). The growth model simulations were conducted after learning was completed. Using Type II as an example, Fig. 3 presents the recalling simulation (prediction) process of the Type II static growth model. The recalling simulation process in Fig. 3 is a static prediction based on a static learning model. The simulation is batch type, and all the DW_{i-1} values must be known in advance from the growth curve. On the other hand, Fig. 4 displays the feedback simulation process of the Type II static growth model. The feedback simulation process in Fig. 4 is a dynamic prediction based on a static learning model. The experimental DW value is an input value only on the first day of the simulation, and the predicted cumulative dry matter weight for the present day (DW_i) is used as the input value for DW_{i-1} on the following day. This acts as a dynamic feedback simulation, and DW_{i-1} can be obtained through the results from the previous day. The simulation process is self starting provided the DW of the initial day of simulation is known.

The learning process in the dynamic growth model is conducted on a daily basis (Fig. 5); twenty-five neural networks are adopted for each growth day from the 6^{th} to 30^{th} day after sowing. The four factors that influence seedling quality are used as the neural network input parameters, namely day temperature (℃), water supply per day per plug tray (mL), total daily solar radiation (mole/m^2), and the DW_{i-1}. The neural network target (prediction) value is DW_i.

All of the networks were combined into a dynamic growth model of the network system after all 25 networks were processed through learning, as illustrated in Fig. 6. Once the DW_0 (DW at the initial day) is known and the first and last days of the growth period are assigned, the dynamic growth model becomes a self starting process for seedling growth simulation. The dynamic learning mode in Fig. 6 is the major feature when compared to the static learning mode with feedback shown in Fig. 4.

RESULTS AND DISCUSSION

The results of the Types I and II static growth models are compared to reveal how the grouping in growth stages influences the model performance. Furthermore, the difference in recalling and feedback simulations by static growth model is discussed, and the dynamic growth model is examined to show its superior performance. The performances of the growth models are evaluated using a relative error and determination coefficient, r^2. The average relative error is defined as follows:

$$\text{Error}(\%) = \frac{\sum_{i=1}^{n} \left| (DW_{pre} - DW_{target}) / (DW_{target}) \right|}{n} \times 100\%$$

where DW_{pre} denotes the DW predicted by the growth model; DW_{target} represents the DW target value; and n is the number of samples.

1. Static Growth Model

Two approaches were employed in the static growth model neural network learning process, according to whether growth stages were considered. Type I combined all the sampled data from six experiments to examine the relationships between environmental factors and

seedling quality using a dual-hidden layer neural network. Meanwhile, Type II exploited sampled data from three distinct growth stages and used one neural network for each stage. The total numbers of learning and testing samples were 2322 and 2302, respectively. Tables 1 and 2 list the analyzed results of recalling simulations for Types I and II. Although the simulated results from both Types were similar, the results from using Type II were slightly better than those with Type I, because the seedlings were expected to share a similar relationship between seedling quality (DW) and growing environment at the same growth stage (Type II, 10 days for each stage). Therefore, the learning scheme with one network for each growth stage helped to improve the accuracy of both training and prediction. In the case that used all DW data, including experimental and interpolated data, the average error exceeded 3.2% for both the Type I and Type II models. The models developed using just end of the growth stage DW data had an average error of below 2.6% (Tables 1 and 2). The error associated with the model's use of real experimental data is expected to be smaller, because the error does not accumulate with time in recalling simulations and experimental data are not interpolated.

Although Tables 1 and 2 showed that the recalling simulation of static growth model had an average error of below 4% and a determination coefficient of over 0.99, it was impossible to practically measure the dry matter weight of seedlings (DW) daily for recalling simulations. The feedback approach illustrated in Fig. 4 was employed to make the simulation more realistic. A feedback approach based on the well-trained static growth model estimated the DW_i and fed it back as the DW_{i-1} for further analysis of each growth day. Table 3 lists the predictions of the static growth model with feedback simulation. The predictions when all DW data from both types are used were similar, with average errors of around 12.5% and determination coefficients at around 0.95. The analyzed results using experimental DW data for Type I had an average error of 16.5%, slightly better than those for type II (18.2%). The error of the feedback simulation in Table 3 is significantly larger than that of the recalling simulation (Table 1 & 2). Consequently, the static growth model with feedback simulation was inadequate compared to the recalling simulation, because the static learning strategy merely adjusted the errors among the sample data which must be known in advance from the growth curve, and not the errors resulting from feeding the estimated output value back as the DW_{i-1}. The feedback simulation produced a large accumulated error because of the static learning scheme being unable to tune the model according to daily changes in growth. The static growth model was trained through the neural network process considering either the whole growth period (Type I) or individual growth stage (Type II), and could not simulate the daily growth such as feedback simulation in Fig. 4. The error was initially small, but accumulated daily and peaked on the last day of each growth stage. Therefore, the error listed in Table 3 for the experimental data was obtained from the maximum error on the last day of each growth stage. On the other hand, the error for all data in Table 3 could be considered the averaged error

over the growth stage. This phenomenon could explain why the error for the experimental data group exceeded that of the whole data group in Table 3.

Regarding the comparison between Types I and II, the results in training and prediction (simulation) both proved that the Type II static growth model performed better overall, as shown in Tables 1-3. However, since models of both Types I and II had an input of DW, which was provided on a daily basis, the difference between the Type II (three networks) and the Type I model (one networks) on the importance of the "growth stage" was reduced. This phenomenon was illustrated by a small difference in the simulation error for all cases in Tables 1-3, and was even not strange to see that Type I gave a better feedback simulation than Type II for experimental data in Table 3 (16.5 vs. 18.2 %), which was an exception among above the cases.

2. Dynamic Growth Model

Although the static growth model in the recalling simulation was quite good (Tables 1 and 2), it was considered impractical, as discussed above. The static growth model in the feedback simulation considered the time feedback, but its predictive ability was inadequate because of its inability to dynamically adjust the daily feedback error. The key to overcoming this shortcoming was to use a dynamic growth model which could adjust the daily feedback error. This approach allowed the daily neural network learning to be fulfilled on a daily basis (Fig. 5). All daily neural networks were then combined in sequence to form a whole dynamic growth model, as illustrated in Fig 6. The dynamic growth model could quickly determine the seedling DW for each growth day via neural network simulation once the DW_0 of the first simulation day and the growth environment conditions were given.

Table 4 lists the simulated daily seedling DW resulting from the dynamic growth model. The daily average error was below 2.9% with a determination coefficient of over 0.98 for the training set samples, while the daily average error was less than 5.8% with a determination coefficient exceeding 0.90 for the prediction set samples. Table 5 lists the lumped results for all growing days. For all data, the average errors of the samples of the training and prediction sets were 1.36% and 3.62%, with determination coefficients of 0.998 and 0.985, respectively. Meanwhile, for the experimental data, the average errors of the samples of the training and prediction sets were 1.68% and 3.75%, with determination coefficients of 0.996 and 0.987, respectively. Comparison of Tables 3 and 5 reveals that the prediction errors decreased by approximately 70% $\sim$ 80% (from 12.4% to 3.62% and from 18.2% to 3.75%), while the corresponding determination coefficient rose from 0.95 (0.92) to 0.99. The dynamic growth model neural network simulation thus performed well owing to dynamic time error minimization.

Figure 7 displays typical estimated growth curves for the static growth model with recalling simulation, the static growth model with feedback simulation, and the dynamic growth model simulation. The Type II approach was used for the static growth model herein. The prediction errors in Fig. 7 for the static growth model with recalling simulation, the static growth model with

feedback simulation, and the dynamic growth model simulation were 3.38%, 23.52% and 4.72%, respectively. The results of the static growth model with recalling simulation results were slightly better than those of the dynamic growth model simulation. The static growth model with recalling simulation performed best in terms of prediction error, but was unsuitable for practical applications because of the unavailability of the daily seedling DW. Unlike its good performance with the recalling simulation, the results of the static growth model for the feedback simulation were the worst among models, with the deviation of the estimated growth curve from target values at each growth stage becoming increasingly obvious with more growing days. Although the corresponding error on the first day of each growth stage (the experimental value as the DW_{i-1} input at the 6th, 11th, and 21st day) was small, the relevant error increased to a maximum on the last day of each growth stage (the 10th, 20th, and 30th day). Although the static growth model with feedback simulation could utilize the dynamic feedback of DW, the static nature of the learning process compromised prediction ability and caused errors to accumulate over time. The estimated growth curve of the dynamic growth model simulation was within a small error range and the error did not increase with the number of growing days, as shown in Fig. 7. Consequently the simulation performance of the dynamic growth model was proven to be good, and the only inputs required for dynamic feedback were the DW_0 at the beginning of simulation and daily environmental conditions. Therefore, the dynamic growth model is suggested as the best of the models presented in this study.

CONCLUSION

This investigation cultivated cabbage seedlings in a phytotron with various environmental conditions (temperature, water supply, and radiation). Experiments involved three growth stages, seedling DW was measured and applied to construct the growth curve by using the cubic spline function.

The feedback neural network simulation benefited from historical growth factors and achieved good learning results when it utilized the DW_{i-1} as an input parameter. The static growth model with recalling simulation was reasonably accurate since it had a 3.6% error for all data groups and a 2.6% error for the experimental data group, but it was impractical because the daily seedling DW was not available in advance. The static growth model with feedback simulation was less accurate than the recalling simulation, with the error of all data groups surpassing 12%, while that of the experimental data group exceeded 16%. The static growth model feedback simulation suffered from a significant accumulated error and could not adjust the daily feedback error.

The dynamic growth model simulation effectively improved the error accumulation by using dynamic feedback learning. The dynamic growth model revealed that the errors of training and prediction sets were 1.68% and 3.75%, with determination coefficients of 0.996 and 0.987 respectively. The dynamic growth model neural network system not only had the advantage of feedback learning, but also performed well in

response to dynamic time error adjustment. This work successfully used a neural network simulation to develop a dynamic growth model that could be used to produce an optimal seedling environment control and automated seedling cultivation strategy.

ACKNOWLEDGMENT

The authors would like to thank the National Science Council, Taiwan for financially supporting this research under Contract No. NSC 89-2313-B-002-238. National Taiwan University is appreciated for providing access to the phytotron. Special gratitude is also extended to those who assisted in experimental work in Lab 405, Dept. of Bio-Industrial Machatronics Engineering, National Taiwan University and Lab 607, Dept. of Agricultural Machinery Engineering, National Chung-Hsing University.

REFERENCES

Chen, S., K. W. Hsieh, and W. H. Chang. 1999. Neural network analysis of sugar content. ASAE Paper No. 99-3083. St. Joseph, Mich.: ASAE.

Elizondo, D. A., R. W. McClendon, and G. Hoogenboom. 1994. Neural network models for predicting flowering and physiological maturity of soybean. *Trans. ASAE* 37(3): 981-988.

Gerald, C. F., and P. O. Wheatley. 1999. Applied Numerical Analysis. 6th Ed. New York, N. Y.: Addison Wesley Longman, Inc.

Hsieh K. W., S. Chen, and J. H. Lai. 1999. Neural network analysis of environmental conditions toward cabbage seedling quality. ASAE paper No. 99-5007. St. Joseph, Mich.: ASAE.

Huang, P. K. 1992. Plug seedling production of horticultural crops. In *Proceedings of Improvement Crop Production*, 163-190. Taichung, Taiwan: College of Agriculture, National Chung-Hsing University.

Jacobson, B. K., J. W. Jones, and P. Jones. 1987. Tomato greenhouse controller: Real-time expert system supervisor. ASAE Paper No. 87-5022. St. Joseph, Mich.: ASAE.

Jones, J. W., E. Dayan, L. H. Allen, H. van Keulen, and H. Challa. 1991. A dynamic tomato growth and yield model (TOMGRO). *Tran.s ASAE* 34(2): 663-672.

Jones, P., J. W. Jones, and Y. Hwang. 1989. Online optimization of heating and CO_2 control in greenhouse tomato production. ASAE Paper No. 89-7020. St. Joseph, MI: ASAE.

Marsh, L. S., L. D. Albright, R. W. Langhans, and C. E. McCulloch. 1987. Economically optimum day temperatures for greenhouse lettuce production. ASAE Paper No. 87-4023. St. Joseph, Mich.: ASAE.

MALAB User's Guide. 1995. Natick, Mass: The Math, Inc.

Murase, H., Y. Nishiura, and N. Kondo. 1992. Neural network model for tomato fruit cracking. ASAE Paper No. 92-3593. St. Joseph, Mich.: ASAE.

Nederhoff, E. M., H. Gizen, and J. Vegter. 1989. A dynamic simulation model for greenhouse cucumber: Validation of

the submodel for photosynthesis. *Acta Hortic.* 248: 255-263.

Seginer, I., A. Angel, S. Gal, and D. Kantz. 1986. Optimal CO_2 enrichment strategy for greenhouse: A simulation study. *J. Agric. Engr. Res.* 34(4): 285-304.

Seginer, I., and R. W. McClendon. 1992. Methods for optimal control of the greenhouse environment. *Trans. ASAE* 35(4): 1299-1307.

Shen, Y., and C. Chang. 1994. Re-analysis and application of a dynamic growth model for pak-choi (*Brassica chinensis*). *Chinese J. Agromet.* 1(2): 63-67.

Whisler, F. D., B. Acock, D. N. Baker, R. E. Fye, H. F. Hodges, J. R. Lambert, H. E. Lemmon, J. M. McKinion, and V. R. Reddy. 1986. Crop simulation models in agronomic systems. *Adv. Agron.* 40: 141-208.

Table 1. Results of Type I (one neural network) static growth model with recalling simulation

Method		Number of Samples	Error (%)	r^2
All data†	Training	2322	3.59	0.999
	Prediction	2302	3.62	0.999
Experimental data at EOGS*	Training	285	2.60	0.999
	Prediction	283	2.60	0.999

† including experimental DW data and the data interpolated from growth curve.

* EOGS : end of growth stages

Table 2. Results of Type II (three neural networks) static growth model with recalling simulation

Method		Number of Samples	Error (%)	r^2
All data†	Training	2322	3.22	0.999
	Prediction	2302	3.24	0.999
Experimental data at EOGS*	Training	285	2.53	0.999
	Prediction	283	2.54	0.999

† including experimental DW data and the data interpolated from growth curve.

* EOGS : end of growth stages

Table 3. Prediction results of static growth model with feedback simulation

Method		Number of Samples	Error (%)	r^2
Type I (one neural network)	All data†	2302	12.6	0.956
	Experimental data at EOGS*	283	16.5	0.923
Type II (three neural networks)	All data†	2302	12.4	0.953
	Experimental data at EOGS*	283	18.2	0.918

† including experimental DW data and the data interpolated from growth curve.

* EOGS : end of growth stages

Table 4. Results of dynamic growth model simulations at each growing day

Growth day	Training			Prediction		
	Number of Samples	Error (%)	r^2	Number of Samples	Error (%)	r^2
6th day	96	0.61	0.999	96	1.05	0.999
7th day	96	0.50	0.999	96	0.83	0.999
8th day	96	0.19	0.999	96	1.06	0.997
9th day	96	0.12	0.999	96	1.03	0.997
10th day	96	0.26	0.999	96	1.67	0.985
11th day	96	0.55	0.998	96	2.33	0.979
12th day	96	1.26	0.993	96	3.13	0.961
13th day	96	1.69	0.988	96	4.05	0.942
14th day	96	1.32	0.992	96	4.20	0.932
15th day	96	1.68	0.990	96	4.37	0.930
16th day	96	1.82	0.988	96	4.66	0.927
17th day	96	2.31	0.986	96	5.05	0.924
18th day	96	2.30	0.985	96	5.17	0.919
19th day	96	2.42	0.984	96	5.40	0.914
20th day	96	2.84	0.982	96	5.75	0.905
21st day	93	1.05	0.996	91	4.27	0.918
22nd day	93	1.20	0.996	91	4.24	0.920
23rd day	93	1.14	0.996	91	4.03	0.922
24th day	93	1.11	0.997	91	4.02	0.925
25th day	93	1.31	0.996	91	4.05	0.926
26th day	93	1.30	0.995	91	3.85	0.933
27th day	93	1.40	0.993	91	3.93	0.935
28th day	77	1.41	0.993	75	4.29	0.933
29th day	77	1.43	0.989	75	4.41	0.933
30th day	77	1.72	0.983	75	4.19	0.940
Weighted Average*		1.36	0.998		3.62	0.985

*. Weighted Average $= \sum_{i=6}^{30} (Average\ Error \times Number\ of\ Samples)_i \div \sum_{i=6}^{30} (Number\ of\ Samples)_i$

Table 5. Simulation results of dynamic growth model

Method		Number of Samples	Error (%)	r^2
All data†	Training	2322	1.36	0.998
	Prediction	2302	3.62	0.985
Experimental data at EOGS*	Training	285	1.68	0.996
	Prediction	283	3.75	0.987

† including experimental DW data and the data interpolated from growth curve.

* EOGS : end of growth stages

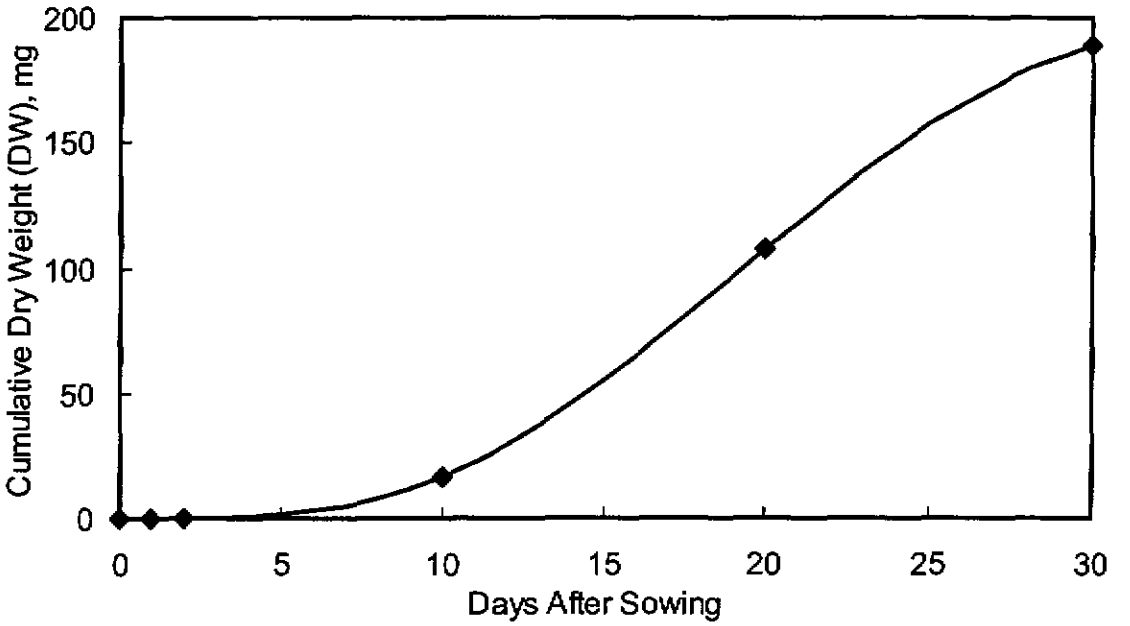

FIG 1. A typical growth curve fitted by cubic spline functions

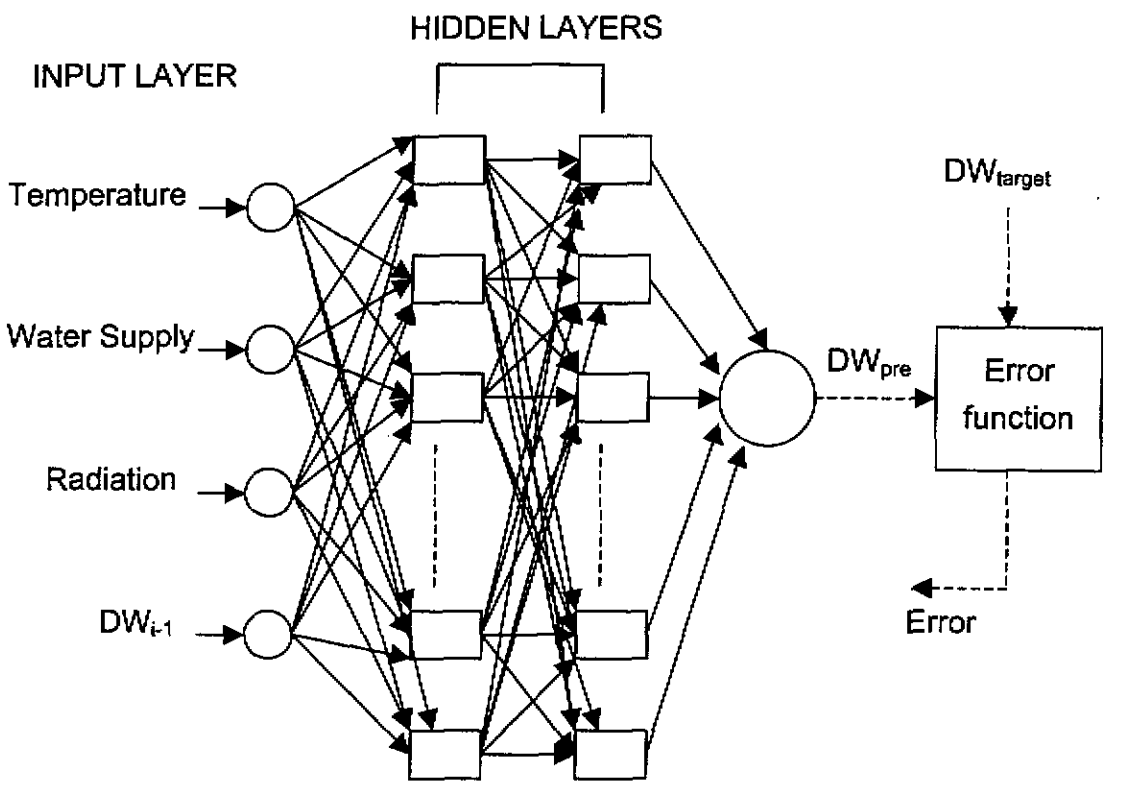

FIG 2. The structure of error-back-propagation neural network

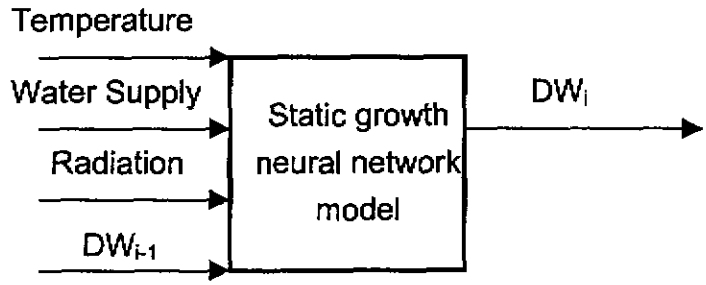

Fig 3. Type II static growth model with recalling simulation process

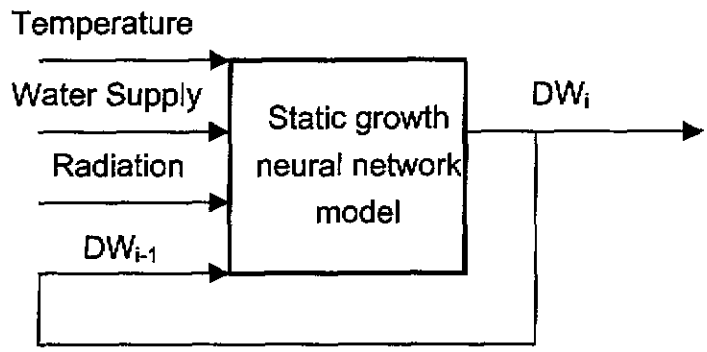

Fig 4. Type II static growth model with feedback simulation process

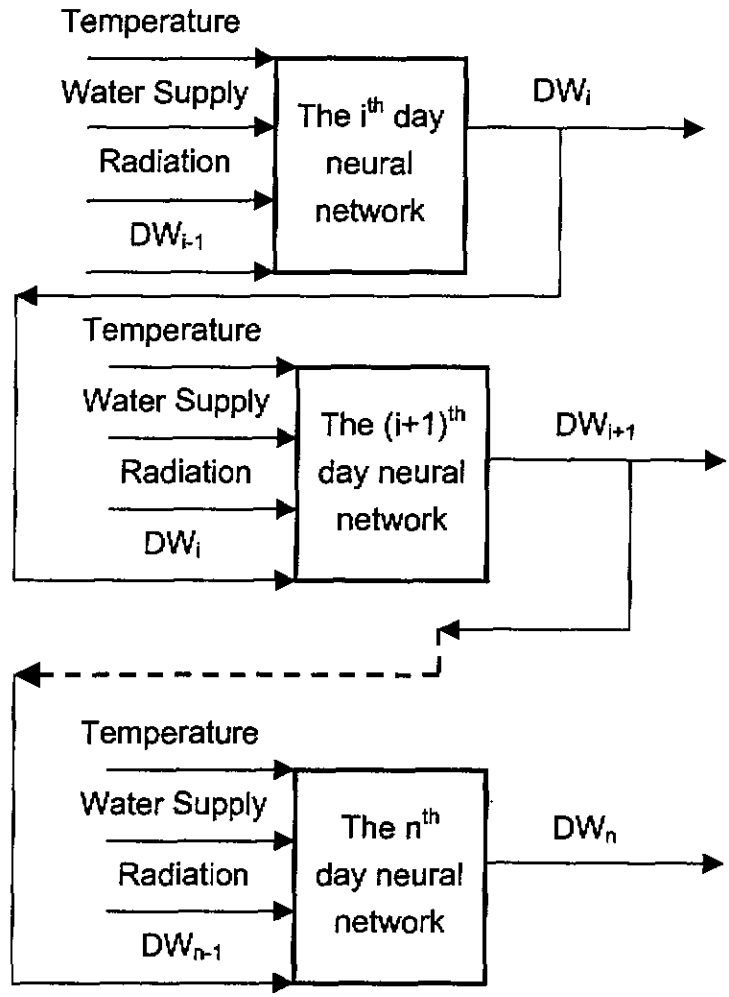

Fig 5. Dynamic growth model in learning process

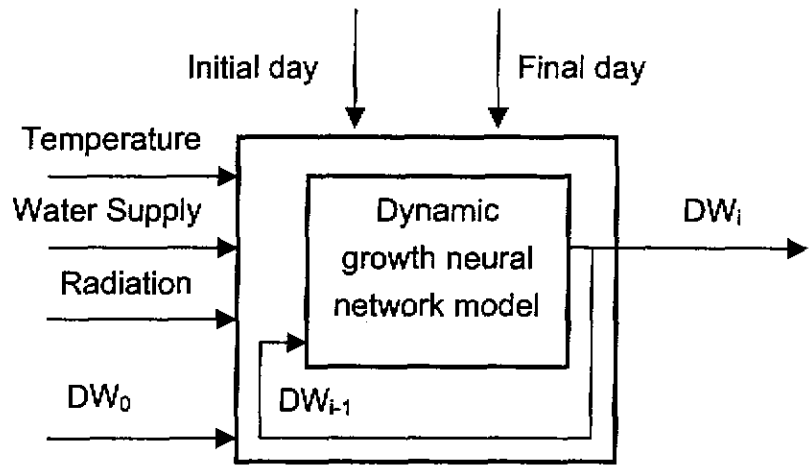

Fig 6. Dynamic growth model in simulation process

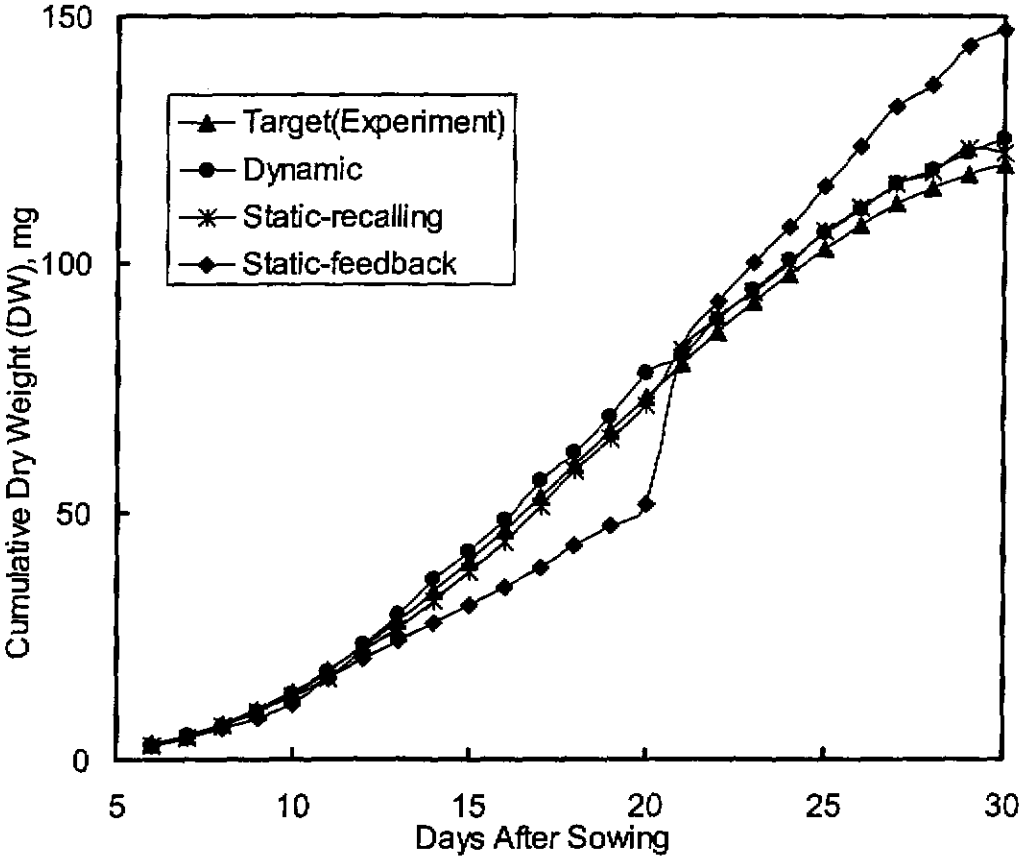

Fig 7. Growth curves predicted by different models